WAVE PROPAGATION OF SINGLE LAYER LATTICE DOMES

by

Akemi NISHIDA[1] and Yasuhiko HANGAI[2]

1. INTRODUCTION

Spatial structure can be classified into continuum system and discrete system(Fig.1.1). With regards to continuum spatial structures such as plate, cylindrical shell, etc., many research works have been presented about their wave propagation behaviours. On the other hand, very few research works have been presented for discrete spatial structures such as lattice dome because of the analytical difficulties due to the existence of many discontinuities. In the stress and the vibration analysis for discrete spatial structures with a lot of members and joints, the continuum analogy method based on the effective stiffness and the effective damping[1] has been developed and widely used in the design process.

Our research objectives are (a) to develop an effective analytical method for the wave propagation of discrete spatial structures, (b) to examine the differences of wave propagation property between continuum and discrete systems and (c) to estimate the effective stiffness and damping which are used in the continuum analogy method from the view point of wave propagation. In this paper, the wave propagation behaviours in single layer lattice domes are analyzed as a first step towards the above research objectives.

Elastic wave theory has been mainly used to investigate the response of structure subjected to impact load or the propagation of earthquake wave. Laplace transform is generally used to analyze the wave equation which is expressed by partial differential equation. But it is not easy to carry out analytically the inverse transform

---

1) Graduate student, University of Tokyo.

2) Professor, Institute of Industrial Science, University of Tokyo

for the solution in the image space except for some special cases. Due to this difficulty, many approximate methods have been proposed ([2] for example). On the other hand, Krings and Waller changed the equation of Laplace inverse transform in such a way that FFT (Fast Fourier Transform) algorithm could be used[3]. Using this method, Adachi et. al. analyzed the impulse response of a finite circular cylindrical shell under the action of longitudinal waterhammer waves[4] and of frame structures in combination with matrix method[5]. Iwasaki, et. al. modified the method by Krings and Waller and proposed a numerical method using both Laplace transform and the finite element method [6]. Doyle has proposed a similar method using Fourier transform instead of Laplace transform (Fig.1.2), and shown that this method is applicable to the analysis of structures with multi degrees of freedom [7]. This analytical method is called the dynamic stiffness method[8-10] and have been used for accurate vibration analysis or non-linear eigenvalue problem. Fukuwa, et.al. used the transfer matrix method to investigate the dynamic characteristics of one dimensional periodic structures and the damping effects due to the joints [11,12].

In the paper, the dynamic stiffness method is used as the numerical method. In order to examine the accuracy of numerical results, wave propagation behaviour of a two dimensional truss structure subjected to impact load is analyzed and compared with results obtained in reference[7]. Next, single layer lattice domes subjected to impact load at the center node are analyzed in order to examine the effect of members in the circumferential direction upon the wave propagation behaviour.

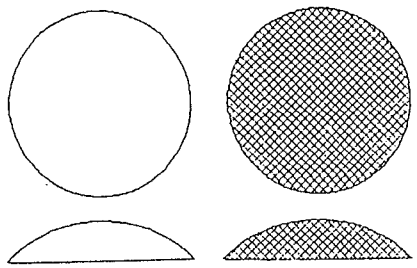

Fig.1.1 Continuum system and discrete system

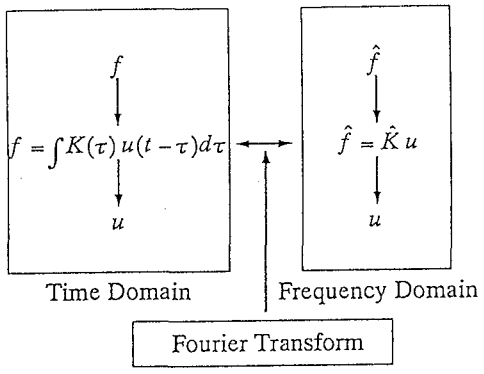

Fig.1.2 Fourier transform

2. SPECTRAL ANALYSIS OF WAVE MOTION IN STRUCTURES

2.1 GOVERNING EQUATIONS FOR A SLENDER ROD

Let us consider a homogeneous, isotropic, linearly, elastic slender rod as shown in Fig.2.1. X axis coincides with the neutral axis of the rod that passes through the centroid of the cross-section. While y and z axes lie on the plane of the neutral surface of the rod, and coincide with the principal axes of the cross-section respectively. Displacements, rotational angles, resultant forces and moments in each direction are represented by u_l, θ_l, P_l and $M_l\,(l=x,y,z)$, respectively. We invoke the basic hypothesis of one dimensional wave theory for longitudinal and torsional motions, and that of Bernoulli-Euler theory of beam for flexural motion. Though Bernoulli-Euler theory is not enough to represent the wave propagation behaviour exactly, it is used here for simplifing the analytical procedure. As a result, the governing equations for the slender rod take the following forms:

longitudinal motion: $$\frac{\partial^2 u_x}{\partial x^2}-\frac{1}{C_0^{\,2}}\frac{\partial^2 u_x}{\partial t^2}=0, \qquad (1\text{-}1)$$

torsional motion : $$\frac{\partial^2 \theta_x}{\partial x^2}-\frac{1}{C_2^{\,2}}\frac{\partial^2 \theta_x}{\partial t^2}=0 \qquad (1\text{-}2)$$

flexural motions : $$\frac{\partial^4 u_y}{\partial x^4}+\frac{1}{C_{by}^{\,2}}\frac{\partial^2 u_y}{\partial t^2}=0,\quad \frac{\partial^4 u_z}{\partial x^4}+\frac{1}{C_{bz}^{\,2}}\frac{\partial^2 u_z}{\partial t^2}=0 \qquad (1\text{-}3)$$

where $$C_0^{\,2}=\frac{E}{\rho},\quad C_2^{\,2}=\frac{G}{\rho},\quad C_{by}^{\,2}=\frac{EI_z}{\rho A},\quad C_{bz}^{\,2}=\frac{EI_y}{\rho A}$$

and E is Young's modulus, G is shear modulus, ρ is mass density, A is cross-sectional area, I_y and I_z are the moments of inertia with respect to y and z axes respectively, and J is the polar moment of inertia($=I_y+I_z$). The resultant forces and moments in each direction are given as follows,

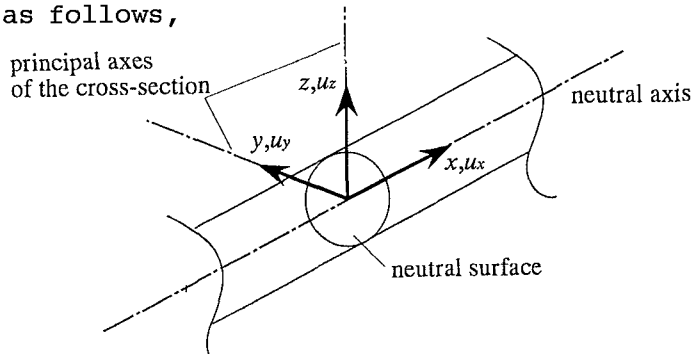

Fig.2.1 slender rod

$$P_x = EA\frac{\partial u_x}{\partial x},\ P_y = -\frac{\partial M_x}{\partial x},\ P_z = \frac{\partial M_y}{\partial x}$$
$$M_x = GJ\frac{\partial \theta_x}{\partial x},\ M_y = -EI_y\frac{\partial^2 u_z}{\partial x^2},\ M_z = EI_z\frac{\partial^2 u_y}{\partial x^2} \qquad (2)$$

Applying the Fourier transform to eqs.(1-1)-(1-3), the following ordinary differential equations can be obtained.

$$\frac{\partial^2 \hat{u}_x}{\partial x^2} + \frac{\omega^2}{C_0{}^2}\hat{u}_x = 0, \qquad (3\text{-}1)$$

$$\frac{\partial^2 \hat{\theta}_x}{\partial x^2} + \frac{\omega^2}{C_2{}^2}\hat{\theta}_x = 0, \qquad (3\text{-}2)$$

$$\frac{\partial^4 \hat{u}_y}{\partial x^4} - \frac{\omega^2}{C_{by}{}^2}\hat{u}_y = 0,\ \frac{\partial^4 \hat{u}_z}{\partial x^4} - \frac{\omega^2}{C_{bz}{}^2}\hat{u}_z = 0 \qquad (3\text{-}3)$$

where $\hat{u}_x$, $\hat{u}_y$, $\hat{u}_z$ and $\hat{\theta}_x$ are the spatially dependent Fourier coefficients. The general solutions of the above equations can be represented by

$$\left.\begin{aligned}
&\hat{u}_x(x,\omega) = \sum_{j=1}^{2} A_j \exp[\lambda_j x],\ \hat{\theta}_x(x,\omega) = \sum_{j=1}^{2} B_j \exp[\zeta_j x] \\
&\hat{u}_y(x,\omega) = \sum_{j=1}^{4} C_j \exp[\eta_{yj} x],\ \hat{\theta}_y(x,\omega) = \frac{\partial \hat{u}_y(x,\omega)}{\partial x} \\
&\hat{u}_z(x,\omega) = \sum_{j=1}^{4} D_j \exp[\eta_{zj} x],\ \hat{\theta}_z(x,\omega) = \frac{\partial \hat{u}_z(x,\omega)}{\partial x}
\end{aligned}\right\} \qquad (4)$$

where

$$\lambda_j{}^2 + k_0{}^2 = 0,\quad k_0{}^2 = \omega / C_0$$
$$\zeta^2{}_j + k_2{}^2 = 0,\quad k_2{}^2 = \omega / C_2$$
$$\eta_{jy}{}^4 - k_{by}{}^4 = 0,\quad k_{by} = \sqrt{\omega / C_{by}}$$
$$\eta_{jz}{}^4 - k_{bz}{}^4 = 0,\quad k_{bz} = \sqrt{\omega / C_{bz}}$$

2.2 LOCAL STIFFNESS MATRIX OF ONE DIMENSIONAL FINITE ELEMENT

Consider a three dimensional frame element of length L as shown in Fig.2.2. This element is identical to that generally used in dynamic finite element analysis except that the mass is evenly distributed along the member instead of concentrated at both ends. Using the general solutions in eq.(4), the displacement shape functions for the element can be represented by

$$\left.\begin{aligned}
\hat{u}_x(x,\omega) &= A_1\exp[-ik_0x] + A_2\exp[-ik_0(L-x)] \\
\hat{\theta}_x(x,\omega) &= B_1\exp[-ik_2x] + B_2\exp[-ik_2(L-x)] \\
\hat{u}_y(x,\omega) &= C_1\exp[-ik_{by}x] + C_2\exp[-k_{by}x] \\
&\quad + C_3\exp[-ik_{by}(L-x)] + C_4\exp[-k_{by}(L-x)] \\
\hat{u}_z(x,\omega) &= D_1\exp[-ik_{bz}x] + D_2\exp[-k_{bz}x] \\
&\quad + D_3\exp[-ik_{bz}(L-x)] + D_4\exp[-k_{bz}(L-x)]
\end{aligned}\right\} \qquad (5)$$

Let us denote nodal displacements and forces at node 1(x=0) and node 2(x=L) in the image space by index subscripts 1 and 2 respectively. Using the condition that the displacements and forces at x=0 and x=L are equal to the nodal displacements and forces, the unknown coefficients A, B, C and D can be evaluated. Then we can get the stiffness equations related to longitudinal, torsional, and flexural motions as follows.

$$\{\hat{f}\} = [K]\{\hat{u}\} \qquad (6)$$

where

$$\{\hat{f}\} = \{\hat{P}_{x1},\ \hat{P}_{y1},\ \hat{P}_{z1},\ \hat{M}_{x1},\ \hat{M}_{y1},\ \hat{M}_{z1},\ \hat{P}_{x2},\ \hat{P}_{y2},\ \hat{P}_{z2},\ \hat{M}_{x2},\ \hat{M}_{y2},\ \hat{M}_{z2}\}^T$$

$$\{\hat{u}\} = \{\hat{u}_{x1},\ \hat{u}_{y1},\ \hat{u}_{z1},\ \hat{\theta}_{x1},\ \hat{\theta}_{y1},\ \hat{\theta}_{z1},\ \hat{u}_{x2},\ \hat{u}_{y2},\ \hat{u}_{z2},\ \hat{\theta}_{x2},\ \hat{\theta}_{y2},\ \hat{\theta}_{z2}\}^T$$

$$[K] = \begin{bmatrix}
s_0\alpha_0 & 0 & 0 & 0 & 0 & 0 & s_0\bar{\alpha}_0 & 0 & 0 & 0 & 0 & 0 \\
 & s_y\alpha_y & 0 & 0 & 0 & s_y\bar{\gamma}_y & 0 & -s_y\bar{\alpha}_y & 0 & 0 & 0 & s_y\gamma_yL \\
 & & s_z\alpha_z & 0 & -s_z\bar{\gamma}_z & 0 & 0 & 0 & -s_z\bar{\alpha}_z & 0 & -s_z\gamma_zL & 0 \\
 & & & s_2\alpha_2 & 0 & 0 & 0 & 0 & 0 & s_2\bar{\alpha}_2 & 0 & 0 \\
 & & & & s_z\beta_zL^2 & 0 & 0 & 0 & s_z\gamma_zL & 0 & s_z\bar{\beta}_zL^2 & 0 \\
 & & & & & s_y\beta_yL^2 & 0 & -s_y\gamma_yL & 0 & 0 & 0 & s_y\bar{\beta}_yL^2 \\
 & & & & & & s_0\alpha_0 & 0 & 0 & 0 & 0 & 0 \\
 & & & & & & & s_y\alpha_y & 0 & 0 & 0 & -s_y\bar{\gamma}_yL \\
 & & & & & & & & s_z\alpha_z & 0 & s_z\bar{\gamma}_zL & 0 \\
 & & & & & & & & & s_2\alpha_2 & 0 & 0 \\
 & & & & & & & & & & s_z\beta_zL^2 & 0 \\
 & & & & & & & & & & & s_y\beta_yL^2
\end{bmatrix}$$

sym.

The detail expressions of each element Kij are given in Appendix. After evaluating the element stiffness matrix for all elements by

eq.(6), the same procedure of conventional matrix method can be used for obtaining the solution. The different point is that it is necessary to compute the solution for all divided discrete frequencies. Upon the application of the Fourier inverse transform to the computed solution, we can then obtain the solution in the real space.

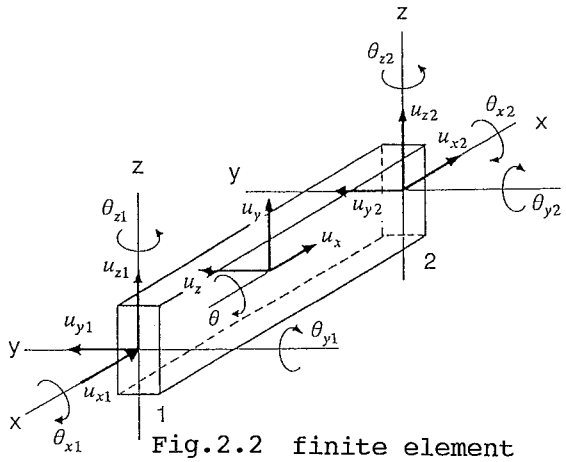

Fig.2.2 finite element

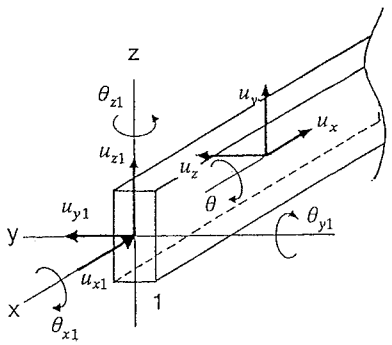

Fig.2.3 semi-infinite element

2.3 LOCAL STIFFNESS MATRIX OF ONE DIMENSIONAL SEMI-INFINITE ELEMENT

As a semi-infinite element of frame, the "Throw-off Element" which could be found in reference[7] is used (see Fig.2.3). The displacements within this element are assumed to be consisted of either only forward moving waves or backward moving waves. Under such assumption, the shape functions of semi-infinite element, corresponding to eq.(5), take the form:

$$\left.\begin{aligned}
\hat{u}_x(x,\omega) &= A_1 \exp\left[-ik_b x\right] \\
\hat{\theta}_x(x,\omega) &= B_1 \exp\left[-ik_t x\right] \\
\hat{u}_y(x,\omega) &= C_1 \exp\left[-ik_{by} x\right] + C_2 \exp\left[-k_{by} x\right] \\
\hat{u}_z(x,\omega) &= D_1 \exp\left[-ik_{bz} x\right] + D_2 \exp\left[-k_{bz} x\right]
\end{aligned}\right\} \qquad (7)$$

In eq.(7), the displacements are assumed to be composed of only forward moving waves. And the governing equations in the image space corresponding to eq.(6) are obtained as follows.

$$\left\{\hat{f}_1\right\} = [K]\left\{\hat{u}_1\right\} \qquad (8)$$

where

$$\left\{\hat{f}_1\right\} = \left\{\hat{P}_{x1},\ \hat{P}_{y1},\ \hat{P}_{z1},\ \hat{M}_{x1},\ \hat{M}_{y1},\ \hat{M}_{z1}\right\}^T$$

$$\left\{\hat{u}_1\right\} = \left\{\hat{u}_{x1},\ \hat{u}_{y1},\ \hat{u}_{z1},\ \hat{\theta}_{x1},\ \hat{\theta}_{y1},\ \hat{\theta}_{z1}\right\}^T$$

$$[K] = \begin{bmatrix} EAik_0 & 0 & 0 & 0 & 0 & 0 \\ 0 & EI_z(i-1)k_{by}^3 & 0 & 0 & 0 & EI_z ik_{by}^2 \\ 0 & 0 & EI_y(i-1)k_{bz}^3 & 0 & -EI_y ik_{bz}^2 & 0 \\ 0 & 0 & 0 & GJik_2 & 0 & 0 \\ 0 & 0 & -EI_y ik_{bz}^2 & 0 & EI_y(i+1)k_{bz} & 0 \\ 0 & EI_z ik_{by}^2 & 0 & 0 & 0 & EI_z(i+1)k_{by} \end{bmatrix}$$

By inserting some semi-infinite elements into the structure to be analyzed, stabilization of numerical computation could be achieved due to the damping effect of semi-infinite element. Also, by using the same means, analysis needed to be carried out only on one part of a large structure could be achieved.

3. NUMERICAl EXAMPLE

- IMPACT RESPONSE OF TWO DIMENSIONAL TRUSS STRUCTURE

In order to examine the accuracy of analysis for multi degrees of freedom structure which contains semi-infinite elements, a two dimensional truss structure which was analyzed in reference [7] was computed using the same condition. The model is illustrated in Fig.3.1. Its members are connected with rotation free joints and torsional and flexural stiffness are not considerd. The material is aluminum with Young's modulus E=10.6$\times 10^6$ lbf/si and mass density ρ=0.0971 lb/ci, where gravity acceleration g is 386.0 in/sec^2. The length of a member L is 5.0 in, and the period of impact loading is 300μs(Fig.3.2).

Time responses of axial force at point A, B, C, D for transform parameters N=1024 and Δt=10μs are shown in Fig.3.3(a) and (b). In these figures, the good agreement between the two analytical results can be seen.

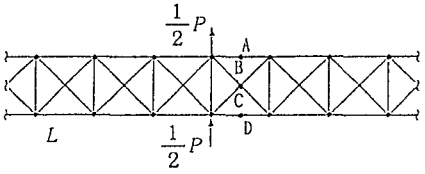

Fig.3.1 Two dimensional truss structure

* Points A, B, C and D are located at the center point of the members. All cross bars are not intersected each other.

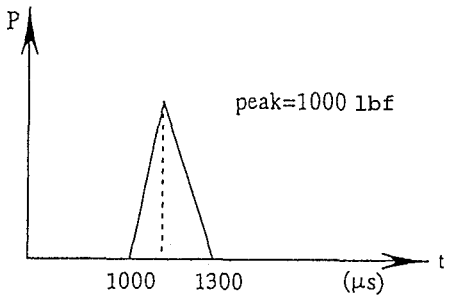

Fig.3.2 Impact load

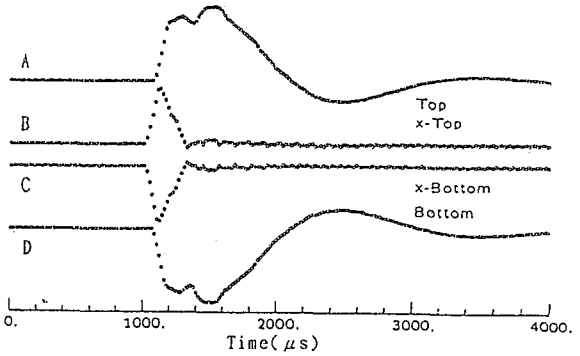

(a) results in reference[7]

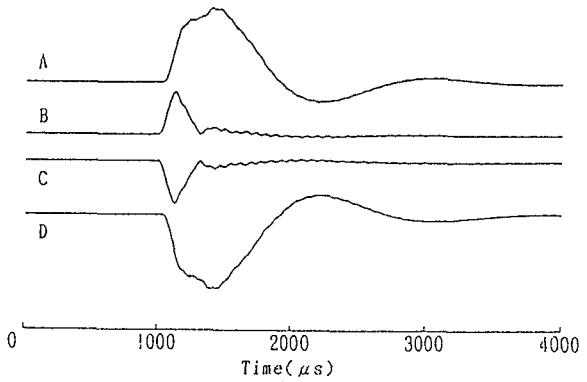

(b) present results

Fig.3.3 Time responses of axial force at point A, B, C and D

4. NUMERICAL ANALYSIS OF SINGLE LAYER LATTICE DOMES

4.1 ANALYTICAL MODELS

A vertical impact load was applied at the central point of a single layer lattice dome with the rise-span ratio of 0.1, and the impact responses were analyzed. As analytical models, two different member arrangement patterns, i.e. pattern 1 and pattern 2, were selected. Three types of models which are different in their member distribution densities were selected for each pattern. And for the purpose of comparing the differences due to the rigidity of joints, the following two types were assumed for the member connections for each of the three models with member arrangement pattern 1, i.e. pinned and rigid joints. Torsional and flexural stiffnesses are not considerd for models with pinned joints. These models are shown in Table 4.1. The material properties and transform parameters used in the computation are shown in Table 4.2 and 4.3 respectively. No damping is considered for models with pinned joints because the continuational time of the responses are short enough for the computational stabilization, while inner damping of 0.5% as in the fol-

lowing form;

$$ {}_d k_{by} = k_{by}(1 - 0.005\, i) \ , \ {}_d k_{bz} = k_{bz}(1 - 0.005\, i) $$

is considered for models with rigid joints for the purpose of stabilizing the computation. The impact load is shown in Fig.4.1.

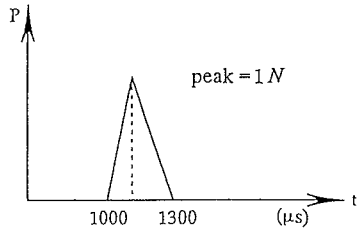

Fig.4.1 Impact load

Table 4.1 Single layer lattice domes

		Type 1	Type 2	Type 3
Pattern 1	Pin	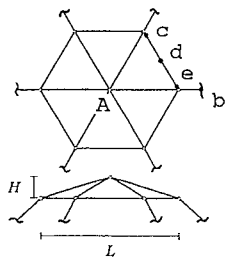	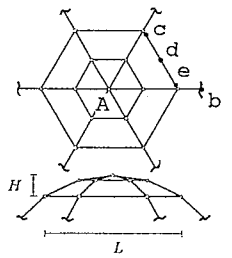	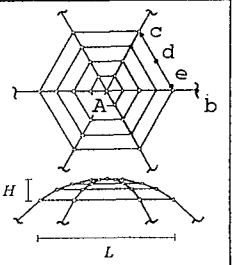
	Rigid	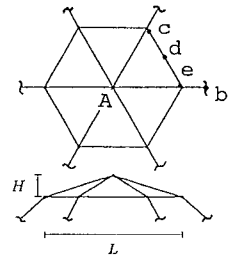	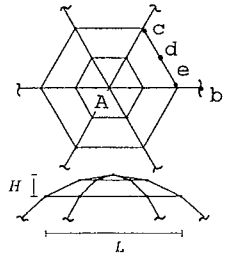	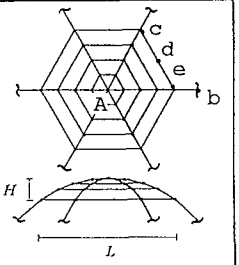
Pattern 2	Rigid	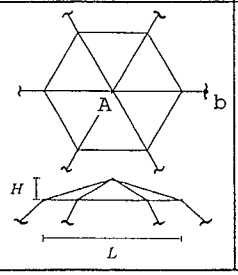	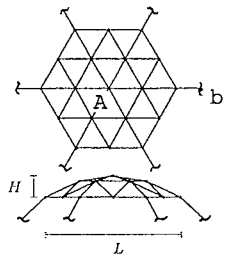	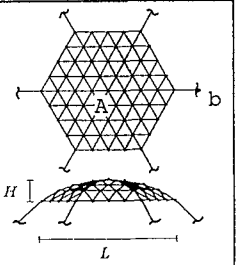
L=50.0cm, H=5.0cm, Cross-sectional shape (Width =0.6cm,Height=0.2cm)				

*1 The dissipated energy to the base part is modeled using six semi-infinite members arranged around each dome.
*2 A is the center point of the dome. The horizontal distance of point b from point A is 0.75L. And point d is a central point of the most external latitude member, while c and e are the two ends of the same member.

Table 4.2 Material properties

Material	Young's Modulus E (N/cm^2)	Poisson's Ratio ν	Shear Modulus G (N/cm^2)	Mass Density ρ (kg/cm^3)
Steel	2.06×10^7	0.29	7.98×10^6	7.85×10^{-5}
Cross-sectional Area A (cm^2)	Moment of Inertia I (cm^4)	Phase Velocity of Longitudinal Wave C_b (m/sec)	Phase Velocity of Torsional Wave C_t (m/sec)	Phase Velocity of Flexural Wave (m/sec)
0.12	Iy=0.0004 Iz=0.0036	5.12×10^3	3.19×10^3	$\sqrt{\omega C_{by}}=172.0\sqrt{\omega}$ $\sqrt{\omega C_{bz}}=298.0\sqrt{\omega}$

Table 4.3 Transform parameters

			N	Δt (μs)	T (μs)	Δf (Hz)	Nyqst freq.(KHz)
Pattern 1	Pin	Type 1	2^{10}(1024)	10	10240	97.656	50
		Type 2			10240	〃	
		Type 3	2^{12}(4098)		40960	24.414	
	Rigid	Type 1	2^{14}(16384)		163840	6.1035	
		Type 2					
		Type 3					
Pattern 2	Rigid	Type 1					
		Type 2					
		Type 3					

4.2 NUMERICAL RESULTS

Firstly, the results obtained by the computation carried out for the three pin-jointed models with arrangement pattern 1 are shown. Fig.4.2 shows the time responses of the vertical velocity at point A. Figs.4.3.1 and 4.3.2 denote the time histories of axial forces and longitudinal velocities at point c,d,e respectively where the symmetrical behaviour about the central point d could be seen. Fig.4.4 shows the time responses of axial force at point b.

In Fig.4.2 , it can be understood that as member distribution density is higher, the maximum values of time responses at point A increase correspondingly. The main reasons are as follows.

1. As the number of joints increases, more reflections and transmissions and also more superpositions of waves occur.
2. As the length of radial member becomes shorter, the angle between two radial members (see Fig.4.5) increases and the local stiffness of the structure decreases.

On the contrary, the maximum time responses at points c,d,e(Fig.4.3.1) and point b(Fig.4.4) decrease and become more complicated with the increase of the density of member distribution. The responses of longitudinal velocity at points c and e in Fig.4.3.2 are completely symmetrical about point d which shows that numerical results are accurate. Furthermore, the longitudinal velocity at point d dose not exist because of the cancellation of waves from the right and the left. The ratios of accumulation of energy flux at point b to external work at pont A are shown in Fig.4.6.

With regards to the continuational time of response after the occurrence of maximum time responses, a longer time period is necessary before a rest condition is achieved as the density of member distribution gets higher as shown in Fig.4.2. This result shows that the density of member distribution strongly influences the wave propagation behaviour. And, as the intervals of member arrangement are closer, higher frequency waves are included in the time responses as shown in Figs.4.2, 4.3 and 4.4.

Secondly, the results obtained by the computation carried out for the three rigid-jointed models with arrangement pattern 1 are shown. Fig.4.7 shows time responses of the vertical velocity at point A. Fig.4.8 shows time responses of axial force at point b.

While it can be seen that the results obtained are similar to that of the pin-jointed models, the differences among the three are not so clear. This is probably due to the reason that wave with a dispersive characteristic can propagate in the rigid-jointed models.

Thirdly, the results obtained by the computation carried out for the three rigid-jointed models with arrangement pattern 2 are shown. Fig.4.9 shows the time responses of the vertical velocity at point A. Fig.4.10 shows the time responses of axial force at point b. It is understood that the waves become smoother when compared with that of the model with arrangement pattern 1 due to the use of members whose length are all the same.

Next, in order to investigate the effect of joint rigidity on wave propagation behaviour, time responses of the vertical velocity at point A for the following models;

(a) pattern 1, Type 1, with pinned joints

(b) pattern 1, Type 1, with fixed joints

have been computed. The results are as shown in Fig.4.11.

Also, in order to investigate the effect of member arrangement pattern on wave propagation behaviour, time responses of the vertical velocity at point A for the following models;

(a) pattern 1, Type 3, with fixed joints

(b) pattern 2, Type 2, with fixed joints

have been computed. The results are as shown in Fig.4.12. Total mass of the above two models are equal.

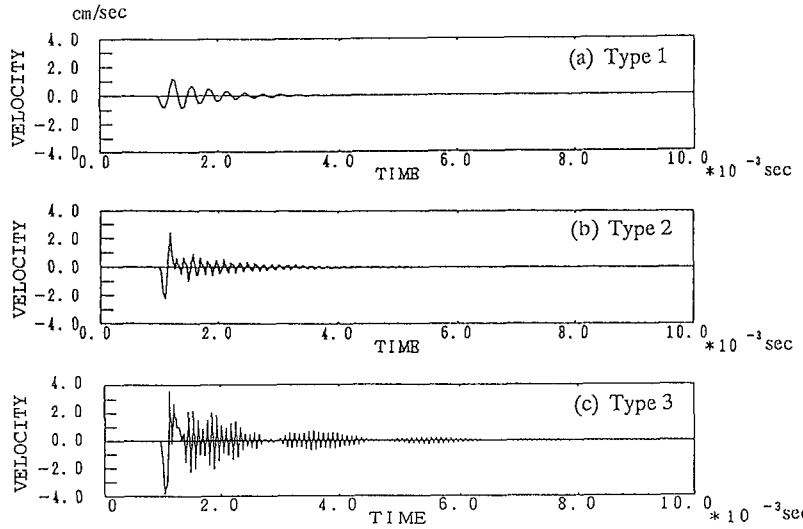

Fig.4.2 Time responses of vertical velocity at point A (Pattern 1, pin-jointed)

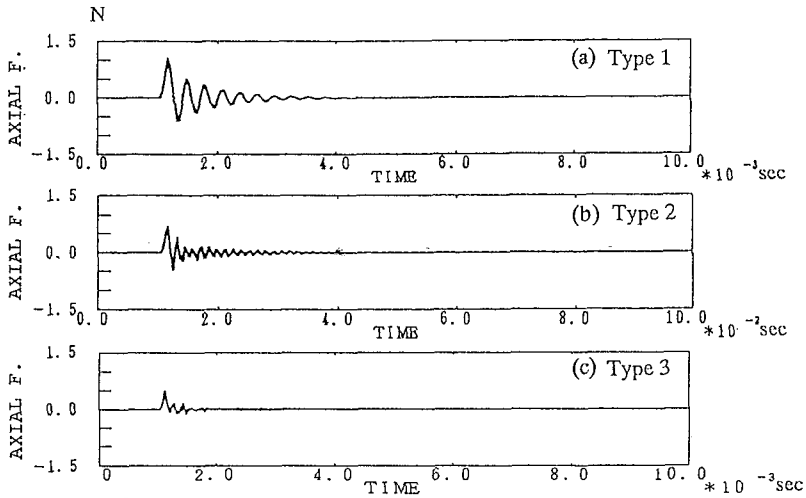

Fig.4.3.1 Time responses of axial forces at point c,d,e (Pattern 1, Pin-jointed)

* The same responces were obtained at the points c and e. The responce of point d is very similar to the two responces, while the differences of the two kinds of responces at the three points c,d,e are not shown clearly.

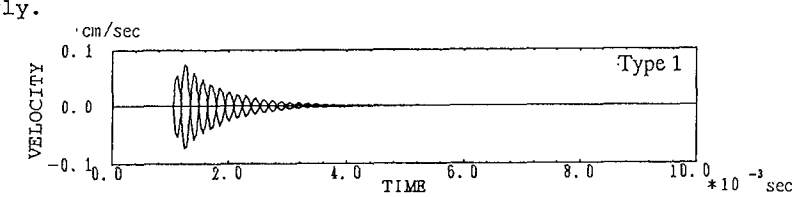

Fig.4.3.2 Time responses of longitudinal velocity at point c,d,e (Pattern 1, Pin-jointed)

* The responses of longitudinal velocity at points c and e are completely symmetrical about point d. Furthermore, the longitudinal velocity at point d dose not exist because of the cancellation of waves from the right and the left.

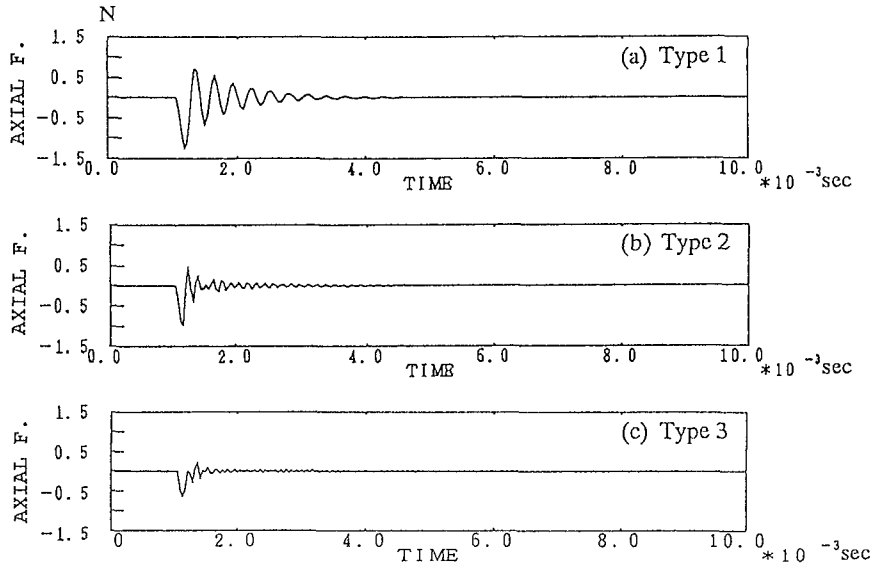

Fig.4.4 Time responses of axial force at point b (Pattern 1, pin-jointed)

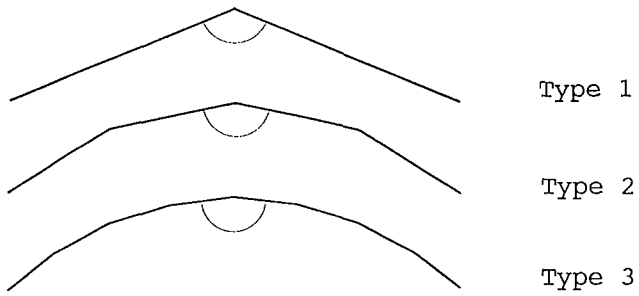

Fig.4.5 The angle between two radial members

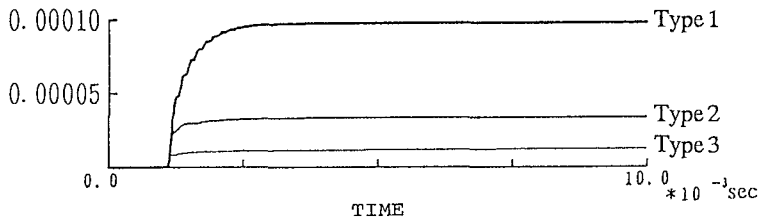

Fig.4.6 Ratios of accumulation of energy flux at point b to external work at point A

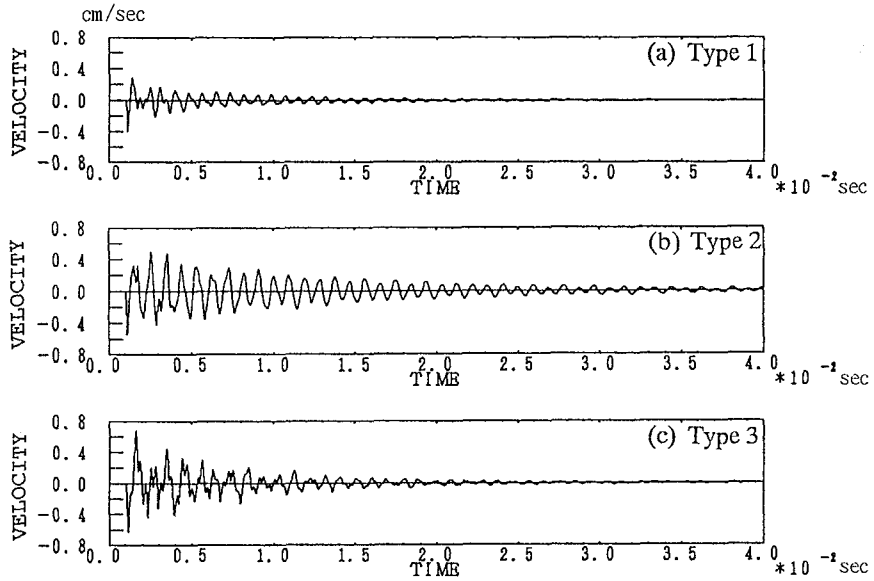

Fig.4.7 Time responses of vertical velocity at point A (Pattern 1, Rigid-jointed)

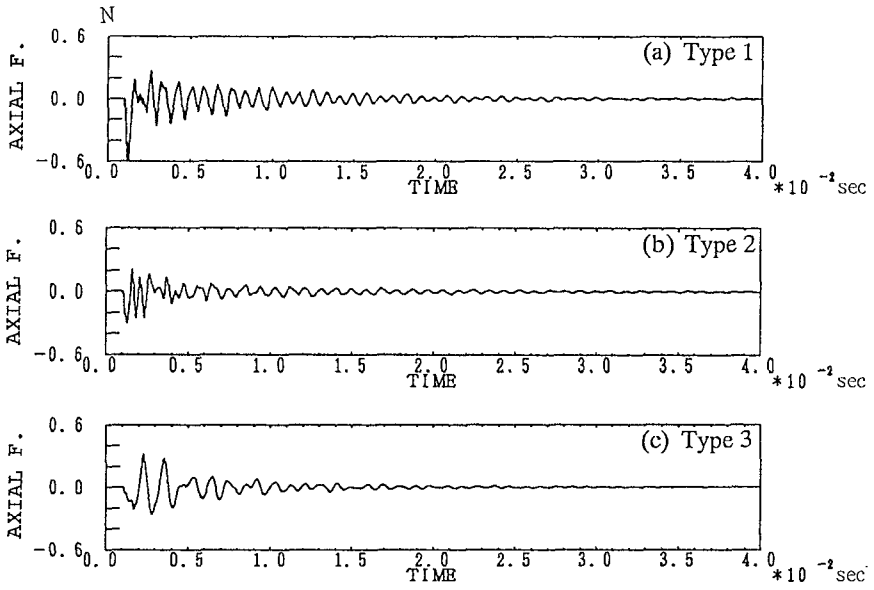

Fig.4.8 Time responses of axial force at point b (Pattern 1, Rigid-jointed)

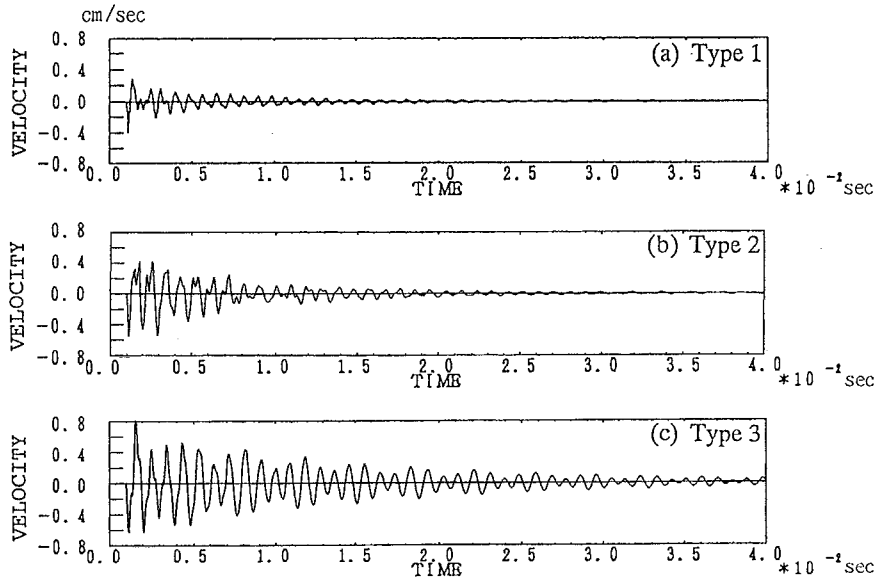

Fig.4.9 Time responses of vertical velocity at point A (Pattern 2, Rigid-jointed)

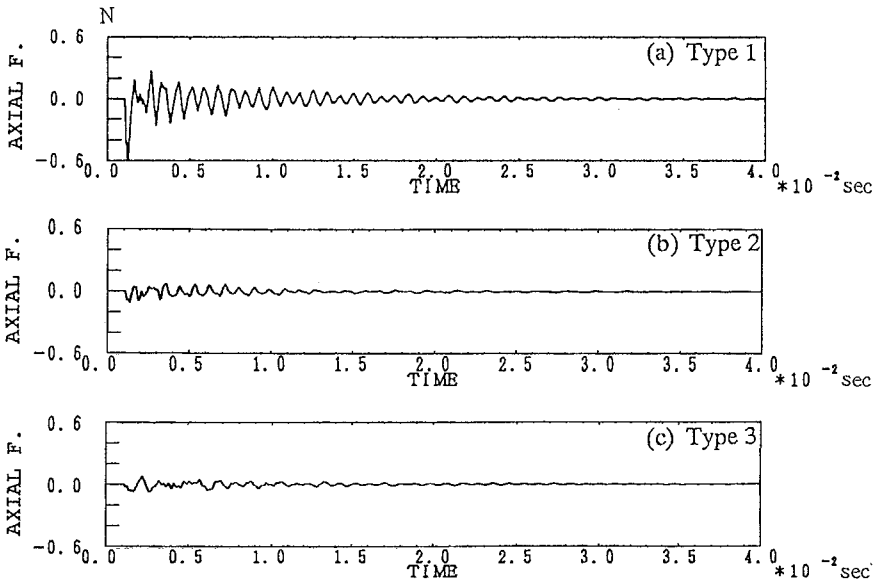

Fig.4.10 Time responses of axial force at point b (Pattern 2, Rigid-jointed)

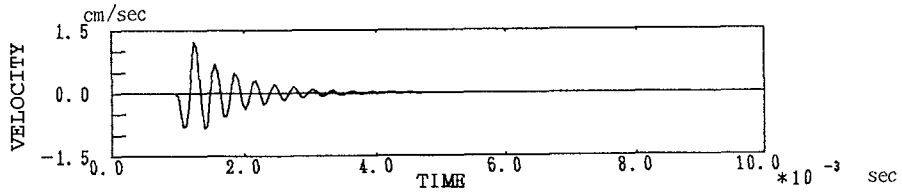

(a) Pattern 1, Type 1, Pin-jointed

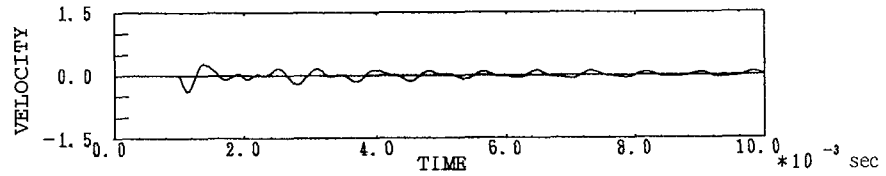

(b) Pattern 1, Type 1, Rigid-jointed

Fig.4.11 Time responses of vertical velocity at point A

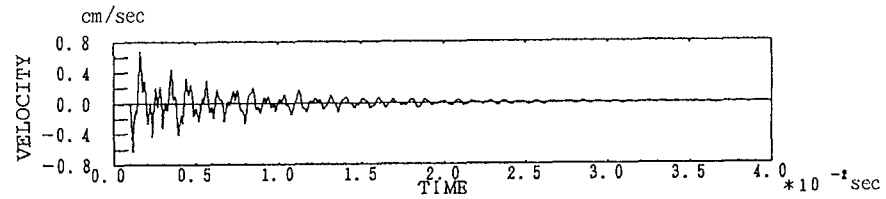

(a) Pattern 1, Type 3, Rigid-jointed

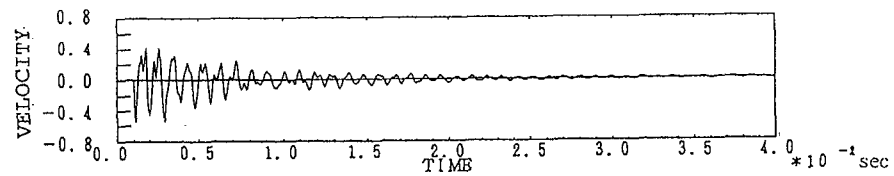

(b) Pattern 2, Type 2, Rigid-jointed

Fig.4.12 Time responses of vertical velocity at point A
(Total mass of these two models are equal.)

5.CONCLUSION

Wave propagation properties in single layer lattice domes subjected to impact load were examined in the paper. Numerical results show that the factors related to member arrangement such as the density, arrangement pattern, rigidity of joints, etc., play an important role upon the wave propagation behaviours. As mentioned in INTRODUCTION, many research works will be required in order to estimate the effective stiffness, the effective damping, and so on, for the continuum analogy method.

REFERENCES

1. Heki, K. et.al. : Space Frames-Design, Analysis, and Construction, Architectural Institute of Japan, 1983.
2. Hosono, T. : Numerical Inversion of Laplace Transform, The Transactions of The Institute of Electrical Engineers of Japan, Vol.99-A, No.64, 1979, pp.44-50.
3. Krings, W. and Waller, H. : Contribution to the Numerical Treatement of Partial differential equations with the Laplace transformation - An application of the Algorithm of the Fast Fourier Transformation, Int. J. Num. Meth. Eng., Vol.14, 1979, pp.1183-1196.
4. Adachi, T. et. al. : Impulsive Response of a Finite Circular Cylindrical Shell due to Waterhammer Waves, Transactions of the Japan Sosiety of Mechanical Engineers, Vol.51-A, No.467, 1985, pp.1886-1892.
5. Adachi, T. et. al. : Impulsive Responses of Framed Structures using a Matrix Method with a Numerical Laplace Transform(1st Report, A Case of Structures Consisting of Straight-bar Elements), Transactions of the Japan Sosiety of Mechanical Engineers, Vol.56-A, No.524, 1990, pp.237-243.
6. Iwasaki, E. et. al. : Transient Response Analysis of Framed Structures using a Laplace Transformation, Journal of Structural Engineering, Vol.38A, 1992, pp.1445-1454.
7. Doyle, J.F.,'Wave Propagation in Structure - An FFT-Based Spectral Analysis Methodology', Springer-Verlag, 1989.
8. Akesson, B.A.,'PFVIBAT-a computer program for plane frame vibra-

tion analysis by an exact method', Int.J.for Numerical Methods in Engng., Vol.10, No.6, 1976, pp.1221-1231.
9. Richards, T.H. and Leung, Y.T., 'An Accurate Method in Structural Vibration Analysis', J. Sound Vibration, Vol.55, No.3, 1977, pp.363-376.
10. Hallaver,Jr.,W.L. and Liu, R.Y.L.,'Beam bending-torsion dynamic stiffness method for calculation of exact vibration modes', J.Sound Vibration, Vol.85, No.1, 1982, pp.105-113.
11. Fukuwa, N. et. al. : A Study on the Dynamic Characteristics of the Periodic Structure using Transfer Matrix Method, Transactions of AIJ, Journal of Structural and Construction Engineering, No.421, 1991, pp.101-108.
12. Fukuwa, N. et. al. : A Study on the Wave Dispersion in the Discrete Analysis Model and a Proposal of Optimal Consistent Mass Ratio, Transactions of AIJ, Journal of Structural and Construction Engineering, No.433, 1992, pp.83-90.

APPENDIX

The detail expressions of each element Kij (in eq.(6)) are given as follow;

$$s_0 = \frac{EA}{L},\ s_2 = \frac{GJ}{L},\ s_y = \frac{EI_z}{L^3},\ s_z = \frac{EI_y}{L^3}$$

$$\alpha_0 = ik_oL\left(1+\exp[-2ik_0L]\right)/\Delta_0,\ \ \bar{\alpha}_0 = -2ik_oL\exp[-ik_0L]/\Delta_0$$

$$\alpha_2 = ik_2L\left(1+\exp[-2ik_2L]\right)/\Delta_2,\ \ \bar{\alpha}_2 = -2ik_2L\exp[-ik_2L]/\Delta_2$$

$$\alpha_y = i(1+i)(z_{11y}z_{22y}+iz_{12y}z_{21y})(k_{by}L)^3/\Delta_y,\ \ \bar{\alpha}_y = i(1+i)(z_{11y}z_{21y}+iz_{12y}z_{22y})(k_{by}L)^3/\Delta_y$$

$$\beta_y = (1+i)(z_{11y}z_{22y}-iz_{12y}z_{21y})(k_{by}L)/\Delta_y,\ \ \bar{\beta}_y = -(1+i)(z_{11y}z_{21y}-iz_{12y}z_{22y})(k_{by}L)/\Delta_y$$

$$\gamma_y = -2z_{11y}z_{12y}(k_{by}L)^2/\Delta_y,\ \ \bar{\gamma}_y = i(z_{11y}^{\ 2}-z_{12y}^{\ 2})(k_{by}L)^2/\Delta_y$$

$$\alpha_z = i(1+i)(z_{11z}z_{22z}+iz_{12z}z_{21z})(k_{bz}L)^3/\Delta_z,\ \ \bar{\alpha}_z = i(1+i)(z_{11z}z_{21z}+iz_{12z}z_{22z})(k_{bz}L)^3/\Delta_z$$

$$\beta_z = (1+i)(z_{11z}z_{22z}-iz_{12z}z_{21z})(k_{bz}L)/\Delta_z,\ \ \bar{\beta}_z = -(1+i)(z_{11z}z_{21z}-iz_{12z}z_{22z})(k_{bz}L)/\Delta_z$$

$$\gamma_z = -2z_{11z}z_{12z}(k_{bz}L)^2/\Delta_z,\ \ \bar{\gamma}_z = i(z_{11z}^{\ 2}-z_{12z}^{\ 2})(k_{bz}L)^2/\Delta_z$$

where

$$\Delta_0 = 1-\exp[-2ik_0L],\ \ \Delta_2 = 1-\exp[-2ik_2L],\ \ \Delta_y = z_{11y}^{\ 2}+z_{12y}^{\ 2},\Delta_z = z_{11z}^{\ 2}+z_{12z}^{\ 2}$$

$$z_{11y} = 1-\exp[-ik_{by}L]\exp[-k_{by}L],\ \ z_{22y} = 1+\exp[-ik_{by}L]\exp[-k_{by}L]$$

$$z_{12y} = \exp[-ik_{by}L]-\exp[-k_{by}L],\ \ z_{21y} = \exp[-ik_{by}L]+\exp[-k_{by}L]$$

$$z_{11z} = 1-\exp[-ik_{bz}L]\exp[-k_{bz}L],\ \ z_{22z} = 1+\exp[-ik_{bz}L]\exp[-k_{bz}L]$$

$$z_{12z} = \exp[-ik_{bz}L]-\exp[-k_{bz}L],\ \ z_{21z} = \exp[-ik_{bz}L]+\exp[-k_{bz}L]$$